

# Transport Theories for Heavy Ion Collisions in the 1 AGeV Regime

E.E. Kolomeitsev<sup>1</sup>, C. Hartnack<sup>2</sup>, H.W. Barz<sup>3</sup>, M. Bleicher<sup>4</sup>, E. Bratkovskaya<sup>4</sup>, W. Cassing<sup>5</sup>, L.W. Chen<sup>6,7</sup>, P. Danielewicz<sup>8</sup>, C. Fuchs<sup>9</sup>, T. Gaitanos<sup>10</sup>, C.M. Ko<sup>6</sup>, A. Larionov<sup>5†</sup>, M. Reiter<sup>4</sup>, Gy. Wolf<sup>11</sup>, J. Aichelin<sup>2‡</sup>

<sup>1</sup> The Niels Bohr Institute, Blegdamsvej 17, DK-2100, Copenhagen, Denmark,

School of Physics and Astronomy, University of Minnesota, Minneapolis, MN-55455, USA

<sup>2</sup> SUBATECH, University of Nantes - IN2P3/CNRS - EMN, F-44072 Nantes, France

<sup>3</sup> Forschungszentrum Rossendorf, D-01314 Dresden, Germany

<sup>4</sup> Institut für Theoretische Physik der Wolfgang Goethe Universität, D-60054 Frankfurt, Germany

<sup>5</sup> Institut für Theoretische Physik der Universität Giessen, D-35392 Giessen, Germany

<sup>6</sup> Cyclotron Institute and Physics Department, Texas A&M University, College Station, TX-77843, USA

<sup>7</sup> Department of Physics, Shanghai Jiao Tong University, Shanghai 20030, China

<sup>8</sup> National Superconducting Cyclotron Laboratory, Michigan State University, East Lansing, MI-48824, USA

<sup>9</sup> Institut für Theoretische Physik Universität Tübingen, D-72076 Tübingen, Germany

<sup>10</sup> Laboratori Nazionali del Sud INFN, I-95123 Catania, Italy

<sup>11</sup> KFKI Budapest, POB 49, H-1525 Budapest, Hungary

† on leave from I.V. Kurchatov Institute, 123182 Moscow, Russia

## Abstract.

We compare multiplicities as well as rapidity and transverse momentum distributions of protons, pions and kaons calculated within presently available transport approaches for heavy ion collisions around 1 AGeV. For this purpose, three reactions have been selected: Au+Au at 1 and 1.48 AGeV and Ni+Ni at 1.93 AGeV.

## 1. Introduction

Heavy ion collisions in the energy range from 50 AMeV to several AGeV are quite complex. The single particle spectra are not isotropic and the anisotropy depends significantly on the centrality of the reaction. With increasing energy one observes the rise and fall of multifragmentation, where multifragmentation means that in each single collision a multitude of intermediate mass fragments is produced. While above  $E_{kin} = 289(1583) MeV$ ,  $\pi$ 's( $K^+$ 's) can be produced in elementary nucleon-nucleon collisions, experiments have shown that in collisions between nuclei Fermi motion and multiparticle effects allow for meson production at energies well below the threshold in an elementary reaction. Finally, nucleons can be excited to resonances which - according to observations in  $\gamma A$  reactions - change their properties in a nuclear environment.

This complexity of the reactions makes it very difficult to link the experimental results in a unique way with the specific underlying physical processes. The challenge to interpret the experimental results was first met by Yariv and Fränkel [1] and Cugnon [2] who took advantage of the increasing computer power at that time and developed the so-called "cascade approach" in which nucleons behave similarly to classical billiard balls and scatter with the free elementary cross sections. This computational approach allowed for completely new insights into the reaction mechanism and allowed for the first time to interpret the nonequilibrium features of the observed spectra. Disregarding binding energy and mean field effects, these approaches have been limited to small systems at higher energies. The extension to lower energies became possible half a decade later with the numerical realization of the Boltzmann-Uehling- Uhlenbeck (BUU) [3] or Vlasov-Uehling-

‡ invited speaker

Uhlenbeck (VUU) [4] approaches which supplemented cascade approaches by the introduction of an attractive mean field and of Pauli blocking, which suppresses collisions if the phase space is already occupied by other nucleons. This made it possible to describe heavy ion reactions down to energies of 20 AMeV. Over the years these approaches became more and more refined as a result of constructive competitions among different groups and many physical questions have been addressed and answered. The pre-equilibrium proton emission has been quantitatively reproduced. It is nowadays established that subthreshold mesons like  $\eta$ ,  $K$  or  $\rho$  are created in elementary collisions, where at least one of the collision partners had gained additional energy in previous collisions. It is further established that resonances are the primary source for the produced pions.

In the meantime, the simulation programs have matured to the level which allows to go even beyond the original goal of describing the elementary reaction features: They are nowadays commonly used as a tool to find out whether the experimental results allow for a determination of physical quantities for which no solid theoretical predictions are available. These quantities include the energy which is needed to compress nuclear matter as well as the properties of resonances and mesons in a hadronic environment.

For the following three reasons it seems to be useful to compare the simulation programs which have been developed over the years:

- 1) The simulation programs are rather complex - consisting of several thousand program lines - and use quite different numerical techniques. Thus, one has to assess whether the different numerical procedures lead to the same results.
- 2) All programs rely on inputs. Those inputs include all the needed elementary cross sections. Among those there are cross sections which are not known experimentally (like those including a baryonic resonance in the entrance channel), and different theoretical implementations have been introduced. It is evident that different elementary cross sections can yield different results.
- 3) In all programs resonances are produced. Their properties in the hadronic environment as well as their time evolution are little known. The programs use different parameterizations for this and it is not a priori evident how those differences influence the final result.

Thus the detailed comparison presented in the present paper may serve as the first step towards a critical assessment of the predictive power of the simulation programs and to identify the features which have to be improved. We would like to mention that some elements towards a future development are already available. Very detailed calculations of the spectral function of kaons in infinite matter have been published [5] and first steps towards describing the time evolution of resonances in matter have been made [8, 6, 7]. These advances, based on the gradient expansion of the Kadanoff-Baym equation, are difficult to formulate for test particles, and further approximations have been shown to be necessary for actual applications [8]. Apart from these approaches there are a couple of studies providing information on the off-shell transition rates [9, 10].

## 2. The simulation programs

In this comparison nearly all the presently available simulation programs have taken part: The simulation program from the Budapest/Rossendorf group [11], the HSD program developed in Giessen by Bratkovskaya and Cassing [12, 13], the simulation program developed by Bratkovskaya, Effenberger, Larionov and Mosel in Giessen [14], the code developed by Danielewicz in Michigan [15], the RVUU approaches of the Texas A&M group [16] and the Munich/Catania/Tübingen group [17]. Besides these true BUU or VUU models, there are several models which are based on the Quantum Molecular Dynamics approach. These n-body approaches allow for the description of fragment production but as far as the observables discussed here they should give the same results. Therefore, we just refer to ref. [18] for the general features and do not discuss the differences here. These simulation models include the IQMD [19] and URQMD [20], both developed in a collaboration between Nantes and Frankfurt, as well as the QMD of the Tübingen group (by Fuchs)[21]. These programs contain a different number of baryonic resonances as can be inferred from table 1. The URQMD code has been developed for higher (SPS to RHIC) energies and includes neither a binding energy for nucleons nor a kaon-nucleon potential but all known mesonic and baryonic resonances. Also its production mechanism for  $K^+$  is different from other approaches. Therefore it is only included to illuminate the differences.

Program	$\tau$	Resonances
Barz	$\tau_{iso}$	$\Delta's, N's$ with $M < 2$ GeV
RVUU (Chen)	$\tau_{iso}$	$\Delta(1232)$
Danielewicz	$\tau_{iso}$	$\Delta(1232), N^*(1440)$
QMD (Fuchs)	$\tau_{iso}$	$\Delta(1232), N^*(1440)$
Gaitanos	$\tau_{iso}$	$\Delta(1232), N^*(1440)$
HSD (Cassing)	$\tau_{iso}$	$\Delta(1232), N^*(1440), N(1535)$
IQMD (Hartnack)	$\tau_{wig}$	$\Delta(1232)$
Larionov	1/120 MeV	$\Delta's, N's$ with $M < 2$ GeV

**Table 1.** The width of the  $\Delta$  resonance and the resonances employed in the programs.

### 3. The Procedure

The simulations programs, which are compared in this article, have been frequently compared with experimental data and usually gave quite satisfying agreement. It is, however, difficult to base program comparisons on those calculations because rarely the same data have been compared with different simulation programs and in the rare cases one has done so, it is not evident that the same experimental filter or the same centrality selection has been employed. To assess the predictive power of these programs and to see whether differences in the predictions are sufficiently large to be experimentally relevant, it is much better to compare the results of the programs directly without any cuts. In addition, all programs employ the impact parameter as an input variable and therefore it is most convenient to compare the results at a given impact parameter. This excludes of course any comparison with experiment. In this publication we concentrate on 3 reactions: Au + Au at 1 and 1.48 AGeV and Ni+Ni at 1.93 AGeV, all at an impact parameter of  $b = 1$  fm as well as the pion yield as a function of the impact parameter. This choice was guided by the available experimental results.

### 4. Protons

The final proton rapidity distribution measures the amount of stopping and reflects how much energy becomes available for particle production. The recent analysis of the FOPI collaboration [22] shows that, in the center of mass system, the variance of the transverse rapidity distribution is always smaller than twice the variance of the longitudinal rapidity distribution even in the most central collisions. If the system were in thermal equilibrium one would expect that the ratio  $R$  of the variances equals one. Experimentally the largest degree of thermalisation ( $R \approx 0.85$ ) is observed for central Au + Au collisions around 400 AMeV. Below that energy Pauli blocking is still too active, while above the NN cross section becomes more and more forward peaked and therefore the energy transfer into the perpendicular directions is lowered. In addition, more energy has to be transferred in order to come to equilibrium. The rapidity and transverse momentum distributions from simulations, figs.1 and 2, reflect this approach to equilibrium. For the heavy systems the final rapidity distributions is peaked at or very close to midrapidity and the simulations differ only little. Initially the protons are located around  $y_{cm} = 0.68, 0.8, 0.89$  for the three reactions, respectively. The resulting rapidity shift for the large systems is thus large. A slightly smaller shift is observed for the light system and there also differences develop between the predictions of the different programs. This kind of differences should be measurable and can help to validate the assumptions made. In transverse direction and on logarithmic scale, we find a general agreement among the programs for Au+Au collisions. However, in the lighter system pronounced differences develop. They seem to be correlated with the rapidity distribution and reflect a different degree of stopping in the different approaches. The differences are most pronounced at small transverse momenta. To fill this part of phase space many collisions are necessary. Therefore its form is a measure for the number of collisions during the interaction. Table 2 summarizes the average squared momenta in the center of mass system at the end of the reaction, along the beam (z) direction and in the direction (y) perpendicular to the reaction plane.

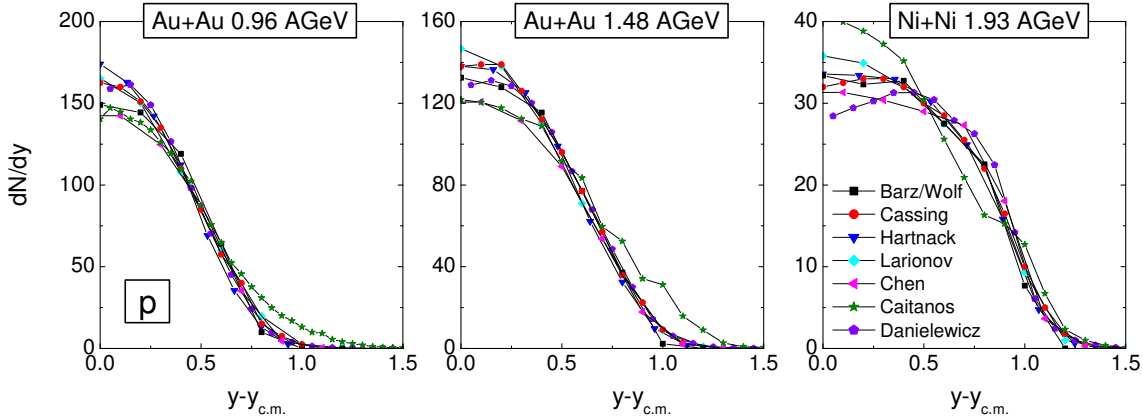


Figure 1. Final proton rapidity distribution at  $b = 1\text{fm}$  in the different approaches

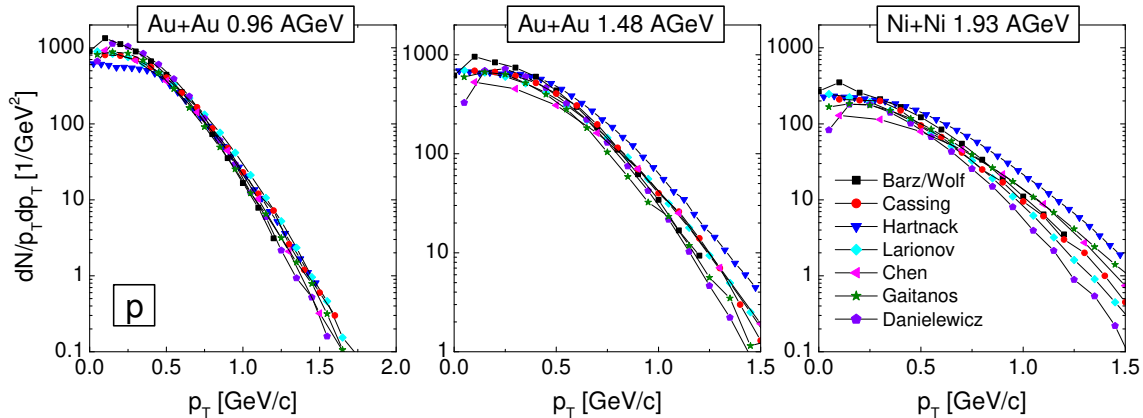


Figure 2. Final proton transverse momentum distribution at  $b = 1\text{fm}$  in the different approaches

Program	1 AGeV Au+Au			1.48 AGeV Au+Au			1.93 AGeV Ni+Ni		
	$\langle p_z^2 \rangle$ (GeV $^2/c^2$ )	$\langle p_y^2 \rangle$ (GeV $^2/c^2$ )	$\frac{\langle p_y^2 \rangle}{\langle p_z^2 \rangle}$	$\langle p_z^2 \rangle$ (GeV $^2/c^2$ )	$\langle p_y^2 \rangle$ (GeV $^2/c^2$ )	$\frac{\langle p_y^2 \rangle}{\langle p_z^2 \rangle}$	$\langle p_z^2 \rangle$ (GeV $^2/c^2$ )	$\langle p_y^2 \rangle$ (GeV $^2/c^2$ )	$\frac{\langle p_y^2 \rangle}{\langle p_z^2 \rangle}$
Barz/Wolf	0.157	0.109	0.69	0.230	0.146	0.64	0.351	0.147	0.42
RVUU (Chen)	0.165	0.121	0.73	0.256	0.172	0.67	0.416	0.172	0.42
Danielewicz	0.162	0.102	0.63	0.257	0.126	0.49	0.407	0.104	0.26
QMD (Fuchs)	0.158	0.111	0.70	0.262	0.138	0.53	0.413	0.107	0.26
Gaitanos	0.131	0.116	0.89	0.240	0.142	0.60	0.300	0.104	0.35
HSD (Cassing)	0.138	0.120	0.87	0.219	0.157	0.72	0.361	0.148	0.41
IQMD (Hartnack)	0.143	0.121	0.85	0.226	0.161	0.72	0.378	0.158	0.42
Larionov	0.163	0.124	0.76	0.252	0.159	0.63	0.405	0.136	0.34

Table 2. Average out-of-plane and longitudinal squared momenta for protons in the different reactions.

## 5. Pions

The direct pion production cross section in nuclear interactions is small. Therefore all pions are created in simulations via resonances. These resonances are produced with the free inelastic NN collisions - which is well known - and in the region of interest comparable to the elastic cross section. In our energy region these are mostly  $\Delta$  resonances which disintegrate into a  $\pi$  and a nucleon. The problem is how to treat this resonance in matter as is required for the simulation programs. The  $\Delta$  resonance, as noted in the particle data booklet, has a width  $\Gamma$  of about 120 MeV and hence

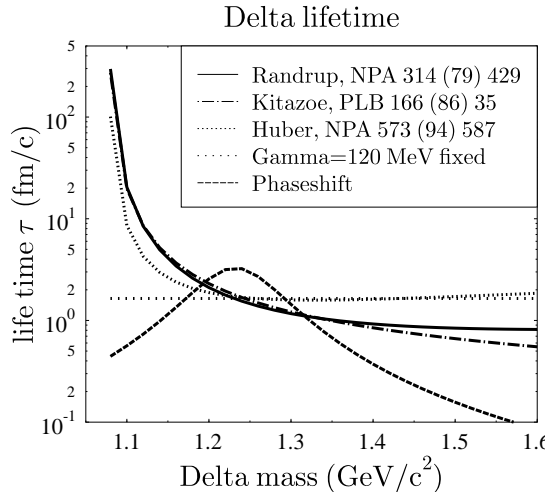


**Figure 3.** The different  $\Delta$  lifetimes which have been proposed.

a lifetime of  $\tau = \frac{1}{\Gamma} = 1.7 \text{ fm}/c$ . Therefore it disintegrates inside the nuclear medium. The width has been determined by analyzing the phase shift in  $\pi N$  scattering as a function of  $\sqrt{s}$ . Around  $\delta(\sqrt{s}) = \pi/2$  the dependence on the energy may be approximated with  $\delta(\sqrt{s}) = \tan^{-1}(\frac{\Gamma}{2(m_\Delta - \sqrt{s})})$ . The lifetime as inverse of a constant width  $\Gamma$  is justified if a) the width were small as compared to the mass difference between the resonance and its decay products ( $\Gamma \ll m_\Delta - (m_N + m_\pi)$ ) and if b) the energy spread of the particle wave packets were large compared to  $\Gamma$ . This is, however, not the case: the nucleons are represented by delta functions in energy. Therefore one has to address the question which lifetime should be assigned to the object which is created in an inelastic nucleon-nucleon collision with a sharp  $\sqrt{s}$  and which yields two nucleons and a pion in the exit channel. There are two approaches in the literature. Ericson and Weise [23], in particular, have analyzed the  $\pi N \Delta$  system in a relativistic isobar model and found for the scattering amplitude

$$f_{33}^\Delta = \frac{\gamma \mathbf{k}^2}{m_\Delta^2 - s - i\gamma|\mathbf{k}|^3}, \quad (1)$$

a form which resembles the usual relativistic Breit-Wigner form and yields an energy dependent  $\Delta$  decay width of

$$\Gamma_\Delta(|\mathbf{k}|) = 2\gamma|\mathbf{k}|^3 = \frac{2f_\Delta^2|\mathbf{k}|^3 M_\Delta}{12\pi m_\pi^2 \sqrt{s}}. \quad (2)$$

With  $f_\Delta^2 = 4.02$  this form reproduces very well the  $\pi N$  data.  $\Gamma_\Delta(|\mathbf{k}|)$  decreases with decreasing  $\sqrt{s}$  and therefore a lifetime defined as

$$\tau_{iso} \propto \frac{1}{\Gamma_\Delta(|\mathbf{k}|)} \quad (3)$$

increases with decreasing  $\sqrt{s}$ .

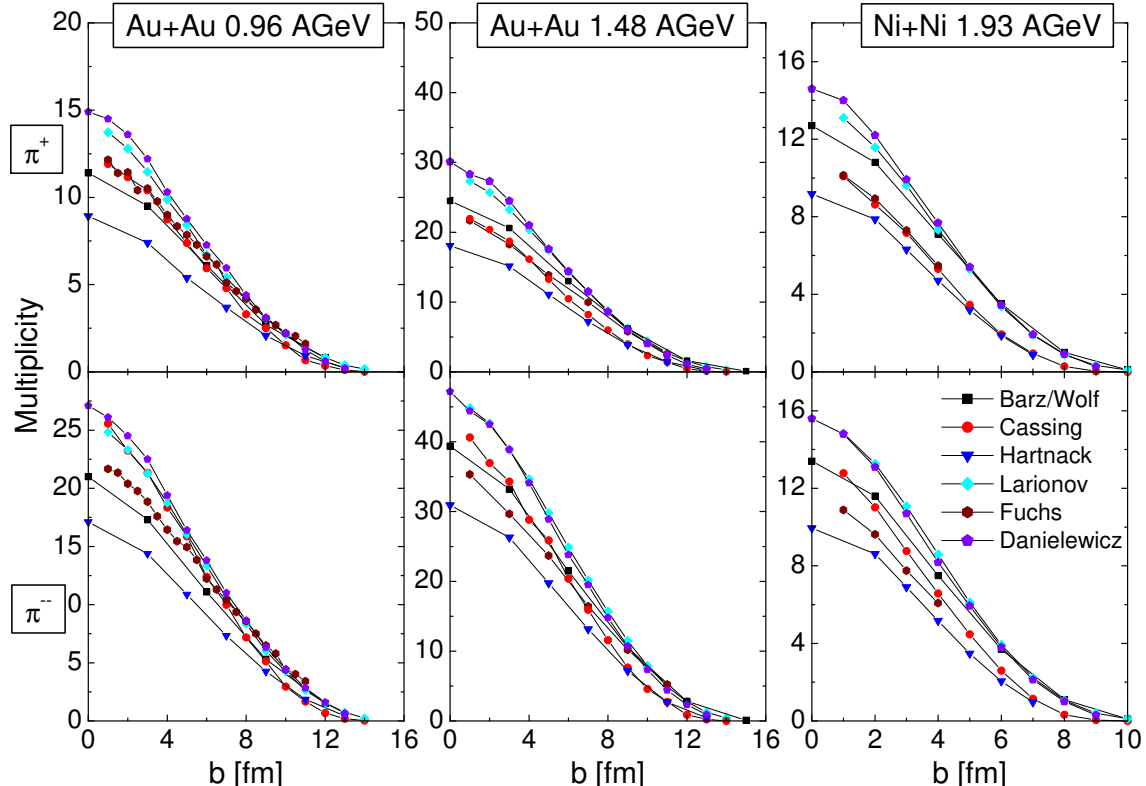
On the other hand, the lifetime of a resonant state has been already analyzed by Wigner [24]. In recent time this considerations have been generalized by Danielewicz and Pratt [25]. They found that quantum mechanically the reaction slows down with a time delay between the outgoing and the incoming wave of

$$\tau_{wig} = 2 \frac{d\delta(E)}{dE}. \quad (4)$$

Hence maximal time delay occurs at the center of the resonance. Fig. 3 show the  $\Delta$  lifetimes in the different approaches as a function of the  $\Delta$  mass. Randrup, Kitazoe and Huber are synonymous for three rather similar approaches which calculate the width using the p-wave scattering amplitude as described above. The description used in the standard versions of the different programs are shown in Table 1.

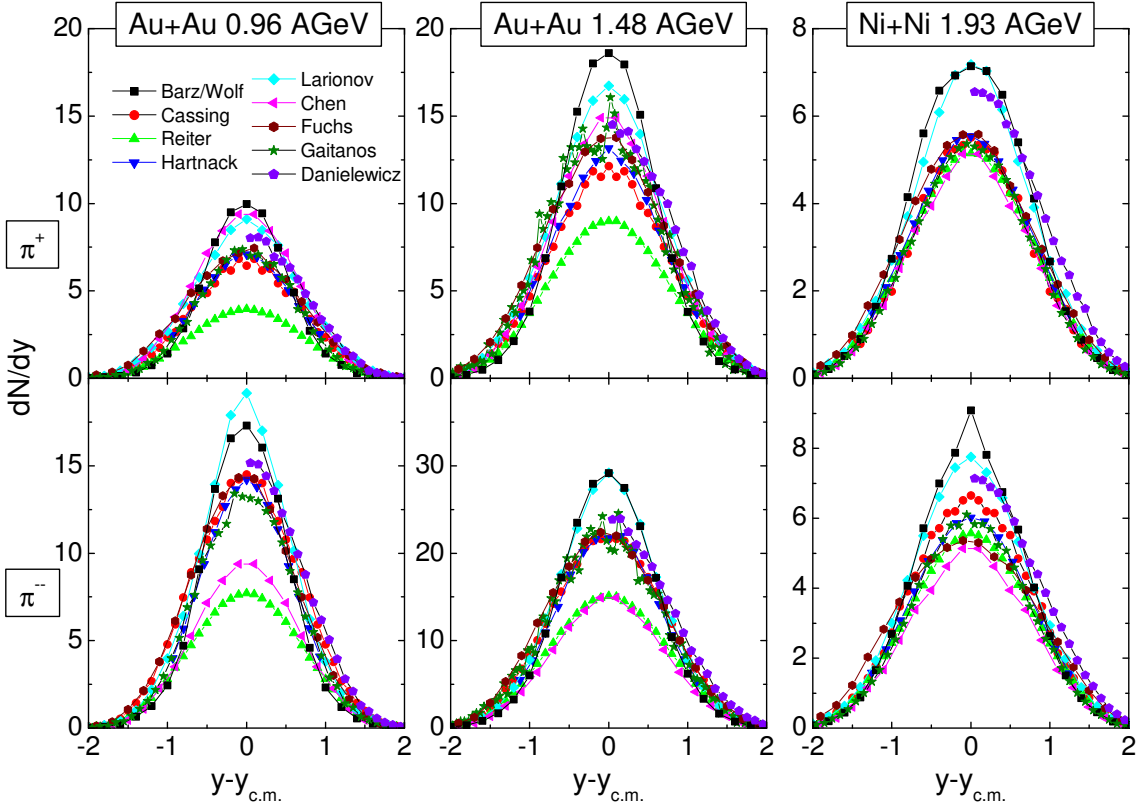
The influence of the choice of  $\tau$  on the final number of pions is by far not negligible. Almost independent of energy and size of the system  $\tau_{iso}$  may yield up to 60% more pions than  $\tau_{wig}$ . If the  $\Delta$  has a short lifetime, several generations of  $\pi$  and  $\Delta$  are produced. In an expanding system the average available center of mass energy in the NN system decreases and the cross section for the production of new  $\Delta$ 's becomes smaller whereas for the backward reaction it is little influenced.

Fig. 4 shows the number of produced pions as a function of the impact parameter for the three reactions. We see the expected significant variations of the total yield. In order to put the



**Figure 4.** Final  $\pi^+$  and  $\pi^-$  multiplicity as functions of the impact parameter in the standard versions of the different approaches characterized by different descriptions of the  $\Delta$  lifetime (see table 1).

results on an equal footing we have decided that all other calculations presented here use a constant lifetime of  $\tau = 1/\Gamma, \Gamma = 120$  MeV. The rapidity and transverse momentum distributions, obtained with this constant lifetime, are displayed in figs. 5 and 6, respectively. We see, first of all, that the differences between the calculations are reduced but not eliminated. The calculation of Reiter, based on URQMD, has to be interpreted with care because in this calculation neither potentials are present nor - being an approach for high energies - special care has been taken to model the inelastic cross section close to threshold. In the program of Chen only the isospin averaged pion yield is available. For that program we have therefore plotted here for  $\pi^-$  and  $\pi^+$  one third of the total  $\pi$  yield. Aside from Reiter's results, the rapidity distributions are rather similar for the majority of the programs. There are, however, some exceptions which show a narrower distribution. The experimental ratio  $R = \pi^-/\pi^+$  at 1 AGeV is close to the value  $R=1.95$  [26] which one expects from the Clebsch Gordon coefficients if (in this neutron/proton asymmetric system) the  $\pi$ 's are exclusively produced via  $\Delta$  resonances. Most of the simulation programs reproduce this value. The slopes of the transverse momentum spectra at midrapidity are very similar as well. The differences concern exclusively  $\pi$ 's with very small  $p_T$  values. This part of the spectra is sensitive to  $\Delta$ 's with a very small mass. We would like to stress that some of the programs include higher ( $N^*$  or  $\Delta^*$ ) resonances whereas others are limited to the  $\Delta$  resonance. This may be of importance at the higher beam energies. Generally the simulation programs seem to overpredict the pion yield. A compilation of the available data in ref. [26] shows an average total pion yield per participant of



**Figure 5.** Final  $\pi^+$  and  $\pi^-$  rapidity distributions at  $b = 1\text{ fm}$  in the different approaches with an enforced  $\Delta$  lifetime of  $1/120\text{ MeV}$ .

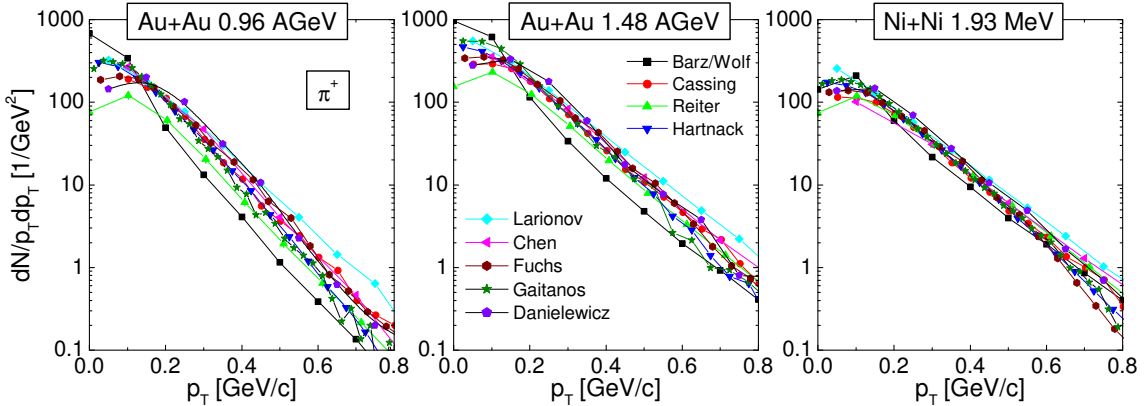


**Figure 6.** Final  $\pi^+$  transverse momentum distribution at  $b = 1\text{ fm}$  and  $|y_{cm}| < 0.5$  in the different approaches with an enforced  $\Delta$  lifetime of  $1/120\text{ MeV}$ .

$\pi^+ + \pi^0 + \pi^- = 1.5(\pi^+ + \pi^-) = 0.075$  and therefore about 30 pions in the most central collisions of Au+Au at 1 AGeV. Please note that the slope of the pion transverse momentum spectra is rather different from that of the protons. This is due the convolution of the  $\Delta$  transverse momentum distribution with its the decay kinematics.

## 6. $K^+$ Mesons

Fortunately, the uncertainty about the optimal description of the  $\Delta$  lifetime influences neither the multiplicity nor the form of the  $K^+$  spectra in a significant way because low mass  $\Delta$ 's have a small cross section to produce a  $K^+$ . Due to the high threshold in the mesonic channel the  $K^+$

are mostly produced in baryon-baryon collisions. To make comparisons more straightforward we enforced for the comparison the same cross sections [27] for the  $N\Delta \rightarrow K^+$  and the  $\Delta\Delta \rightarrow K^+$  channels in the different codes. These cross sections are dominant at  $E_{kin} \geq 1.5 \text{ AGeV}$ . Therefore, and due to the constant  $\Delta$  lifetime, the results presented here may differ from already published results. For the  $NN \rightarrow K^+$  cross section we kept the original cross sections of the programs. For the channel  $pp \rightarrow K^+$  new data at low energies are available [28]. In addition there is the problem of how to extrapolate this  $pp$  cross section to the  $nn, np \rightarrow K^+$  channels. Usually this extrapolation is done by assuming that the  $K^+$  is accompanied by a  $\Lambda$  and that only the isospin coefficients change. In the case of the  $K^+$  this is, however, not so easy because this extrapolation depends on whether a kaon or a pion is exchanged. For the case of a pion exchange we find  $\sigma(np \rightarrow K^+) = 5/2 \sigma(pp \rightarrow K^+)$  and consequently  $\sigma(NN \rightarrow K^+) = 3/2 \sigma(pp \rightarrow K^+)$ ; in the case of a kaon we find  $\sigma(pp \rightarrow K^+) = 2\sigma(np \rightarrow K^+)$  and therefore  $\sigma(NN \rightarrow K^+) = 1/2 \sigma(pp \rightarrow K^+)$ . Very recent data [29] point, however, towards a  $\sigma(np \rightarrow K^+)/\sigma(pp \rightarrow K^+)$  ratio of 3-4. A further complication is the production of the  $K^+$  in the  $pp \rightarrow K^+ N\Sigma$  channel, which has been found to be small [28], but this might be a consequence of the final state interaction. The different  $\sigma(BB \rightarrow K^+)$  cross sections employed are presented in fig. 7 and Table 3. Top panels of

Program	$\sigma(NN \rightarrow K^+)$	$\sigma(N\Delta \rightarrow K^+)$	$(\sigma\Delta\Delta \rightarrow K^+)$
Barz	[27]	[27]	0
Chen	[27]	[27]	[27]
Fuchs	[30] ( $\Lambda$ ) [27] $\Sigma$	[27]	[27]
Gaitanos	[30] ( $\Lambda$ ) [27] $\Sigma$	[27]	[27]
HSD (Cassing)	[12]	[27]	[27]
IQMD (Hartnack)	[30] ( $\Lambda$ ) [27] $\Sigma$	[27]	[27]
Larionov	[27]	[27]	[27]

Table 3. The  $K^+$  cross sections used in the programs.

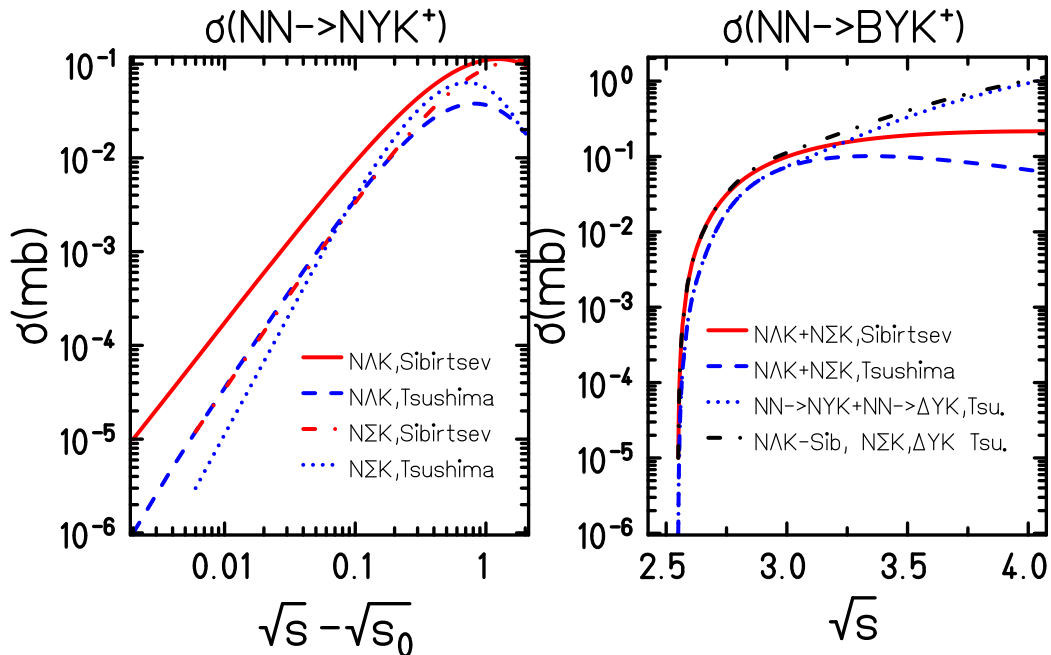
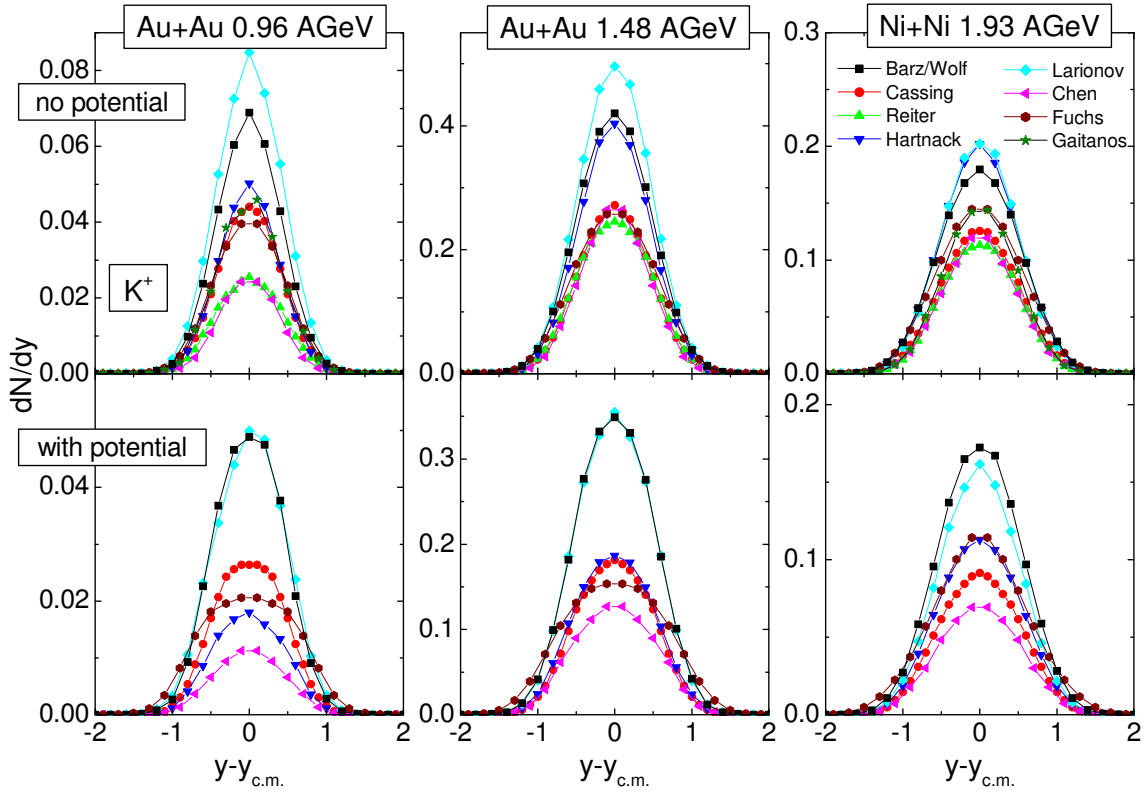


Figure 7. The isospin averaged cross sections  $NN \rightarrow K^+$ .

fig. 8 and fig. 9 present, respectively, the  $K^+$  rapidity and transverse momentum distribution obtained for those cross sections. Also here the URQMD calculations (Reiter) cannot directly be compared with the others. In this approach, the  $K^+$  are created by two body resonance decays



**Figure 8.** Final  $K^+$  rapidity distribution at  $b = 1$  fm and with an enforced  $\Delta$  lifetime of 1/120 MeV (top row without, bottom row with KN potential) in the different approaches.

whereas in all other approaches the  $K^+$  production is a process with three bodies in the final state:  $BB \rightarrow K^+ \Lambda(\Sigma)B$ . We see that URQMD is not suited for 1 AGeV but already at 1.5 AGeV it describes the spectra in a reasonable way although spectra measured in elementary collisions point towards a three - body process. In order to understand the 50% differences of the predictions one has to realize that the  $K^+$  are produced at subthreshold energies in the Au+Au collisions. Therefore the nucleons, which are involved in the  $K^+$  production, had already collisions before. This encodes in the production yield the whole history of the reaction. In addition, the  $K^+$  production cross section rises exponentially close to the threshold and therefore small differences in the parametrization of the Fermi motion of the nucleons or in the potential of the hyperon change the cross section considerably. Some programs contain, in addition, the channel  $\pi B \rightarrow Y K^+$ , but usually this channel does not contribute a lot at these energies due to its large threshold and the few pions as compared to baryons.

Kaons change their properties in the medium. This is the prediction of many theoretical approaches which range from chiral perturbation theory to Nambu Jona-Lasinio model calculations [31]. All these theories should give reliable predictions if the density is low but suffer from the fact that the extrapolations to higher densities are less and less well founded. For our purpose, it is sufficient to parametrize the density dependence by

$$\omega_K(\rho_B, k) = \sqrt{m_K^*(\rho_B)^2 + k^2}, \quad (5)$$

where the effective mass is

$$m_K^*(\rho_B) = m_K^0 \left( 1 - \alpha \frac{\rho_B}{\rho_0} \right), \quad (6)$$

with  $\rho_B$  and  $\rho_0$  being the baryon density and the normal nuclear matter density, respectively. Table 4 displays the different values of  $\alpha$  employed in the calculations: It has been suggested in ref. [32] to compare the ratio  $\frac{d\sigma^{pC}}{dp_t} / \frac{d\sigma^{pA}}{dp_t}$ , which has been measured [33], with calculations using different  $K^+N$  potentials [33], to fix the  $K^+$  potential at normal nuclear matter density.

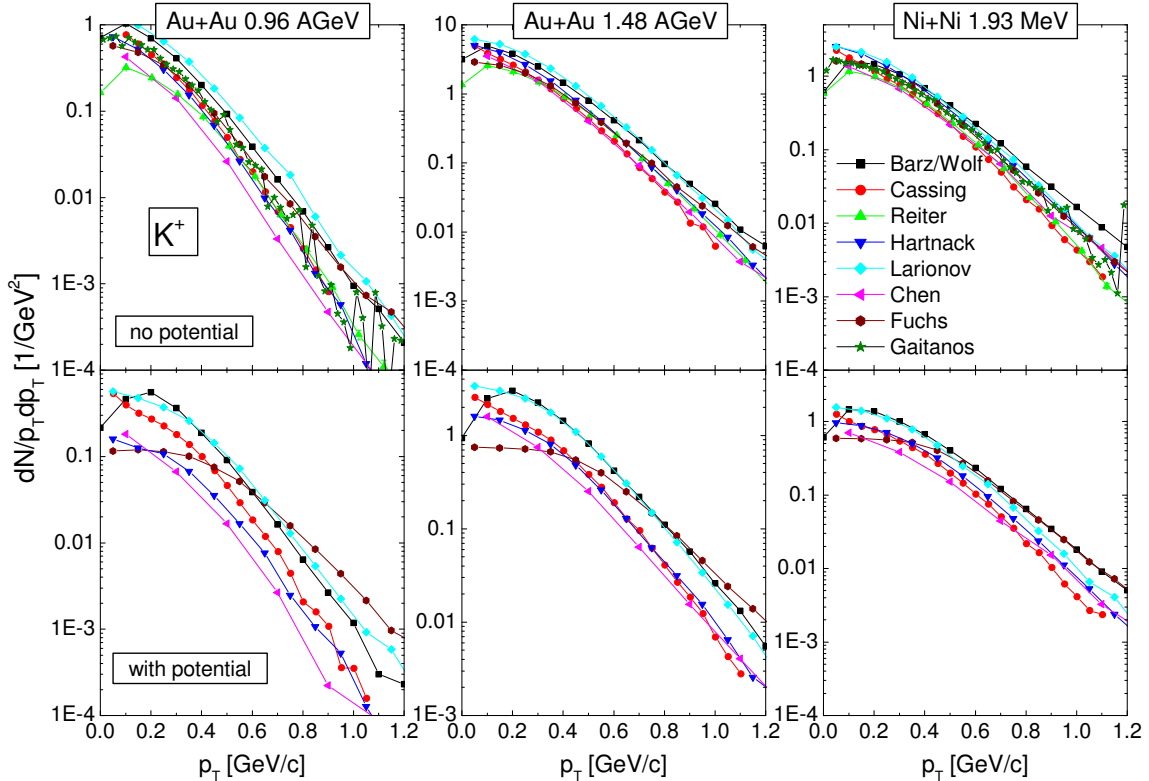


**Figure 9.** Final  $K^+$  transverse momentum distribution at  $b=1$  fm,  $|y_{cm}| < 0.5$  and with an enforced  $\Delta$  lifetime of  $1/120$  MeV (top row without, bottom row with KN potential) in the different approaches.

Program	$\alpha$ [MeV] for $K^+$ ( $K^-$ )
Barz	-0.05 (0.16)
Chen	-0.04 (0.22)
Fuchs	-0.07
HSD (Cassing)	-0.04 (0.10)
IQMD (Hartnack)	-0.075 (0.22)
Larionov	-0.06 (0.2)

**Table 4.** Parameters for the density dependence of the in medium kaon masses  $m_K^*$  (eq.6).

Despite of the moderate increase of the  $\omega_{K^+}(k=0)$  with density, the potential changes the  $K^+$  yield considerably, as one sees in figs. 8 and 9. This is due to the fact that kaons are produced at high density when the mean-free-path is short and therefore the  $\Delta$ 's have a higher chance to collide with a nucleon. Depending on the density dependence of the potential, we see a decrease of the total  $K^+$  yield of about a factor of 2 for the heavy systems and less for the light system if the potential is switched on. The form of the transverse momentum distribution by Fuchs differs from those from other calculations because he uses a covariant form of nuclear current instead of only its forth component, the baryon density, as the other approaches.

The elementary  $K^+$  creation process is azimuthally isotropic. It has been argued that the azimuthal distribution of the  $K^+$  contains information on the  $K^+$  nucleon potential [34]. This is based on the fact that  $K^+$  emitted into the azimuthal angle  $\phi = 90^\circ$  come from highly compressed matter whereas those being emitted near  $\phi = 0^\circ(180^\circ)$  have traversed the cold spectator matter. Therefore one expects an enhancement around  $\phi = 90^\circ$  due to the more repulsive potential. Such an effect may, however, be superimposed by the consequence of the different path lengths in matter. Fig.10 shows the result. The majority of the programs produce a different azimuthal distribution without (top row) and with (bottom row)  $K^+N$  potential. Without the potential, the distribution

is more isotropic and the expected enhancement is seen if the repulsive potential is active.

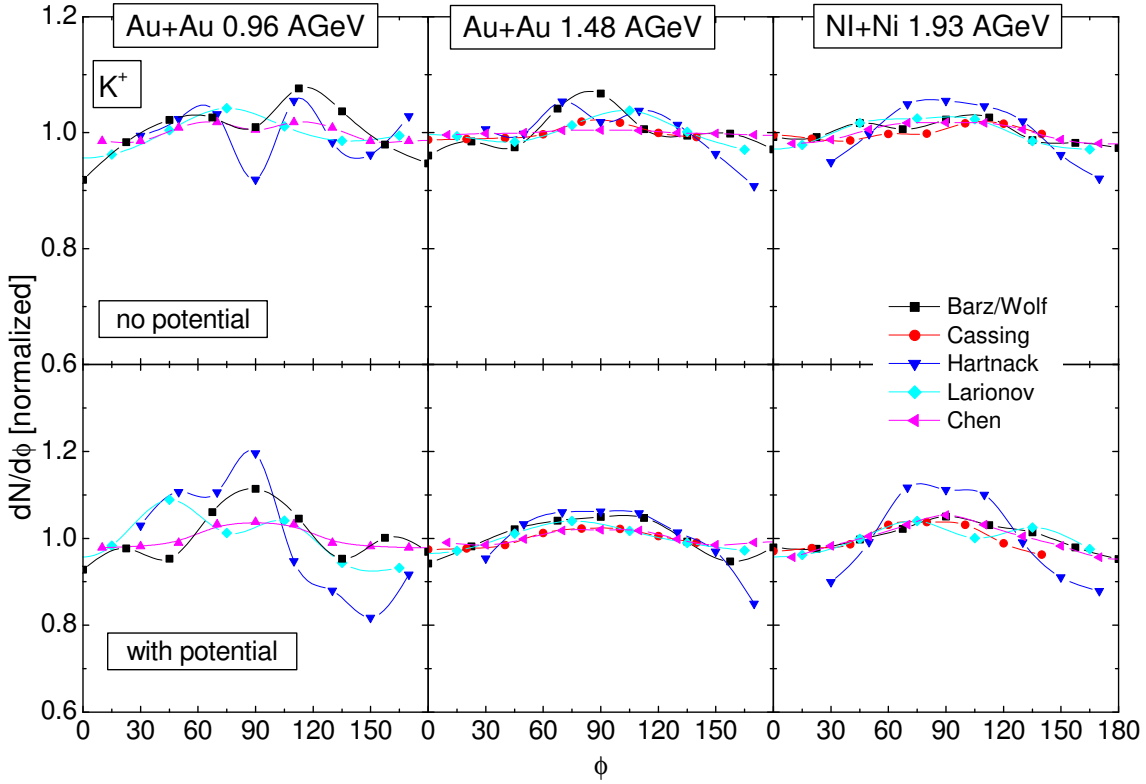


**Figure 10.** Final  $K^+$  azimuthal distribution at  $b=5$  fm,  $|y_{cm}| < 0.5$  and with an enforced  $\Delta$  lifetime of  $1/120$  MeV (top row without, bottom row with KN potential) in the different approaches.

## 7. $K^-$ Mesons

The production process for the  $K^-$  mesons in nuclear reactions is much more complex than that for the  $K^+$ . The reason for this is their s quark content. On the one hand it is much harder to produce a  $K^-$  in elementary pp reactions because of its higher threshold ( $E_{Kin} = 2.513$  GeV for  $pp \rightarrow K^+K^-pp$ ), and on the other hand a  $K^-$  can exchange its s quark with strange baryons ( $K^-N \rightarrow \Lambda(\Sigma)\pi$ ). The cross sections for these exothermic reactions are very large. The inverse reaction  $\Lambda(\Sigma)\pi \rightarrow K^-N$  has been identified as the dominant source of the  $K^-$  production in heavy ion reactions at the energies we consider here [35]. This process is absent in elementary pp interactions and therefore the  $K^-$  yield in heavy ion collisions is orders of magnitudes larger than that in pp collisions for energies not too far away from the threshold. This process couples the  $K^-$  to the  $\Lambda(\Sigma)$  and hence to the  $K^+$  production [36, 37, 38] and explains therefore the experimental observation [39] that the  $K^+$  to  $K^-$  ratio is independent of the impact parameter. The  $K^-$  production in baryon-baryon interactions suffer from the large threshold and takes place only early when the system is dense. Thereafter the  $K^-$  gets easily reabsorbed. In figs. 11 and 12 we display the  $K^-$  rapidity and transverse momentum distributions. The URQMD calculations suffer from the fact that they produce too few strange baryons (produced in the  $BB \rightarrow K^+Y$  reactions) as can be seen from the low  $K^+$  multiplicity. The  $K^-$  channel confronts the simulation programs with the challenge to calculate the  $K^-N$  and the  $\Lambda\pi$  cross sections at values of  $\sqrt{s}$  which are in free space below the threshold. These problem has been solved differently by the different groups.

In view of the complexity of the production processes, the results of those codes, which can be directly compared, are rather similar, especially at higher energies. At higher energies, the transverse momentum distributions are also rather similar. At lower energies the HSD code produces a somehow softer distribution. Also the  $K^-$  changes its properties in the medium. As

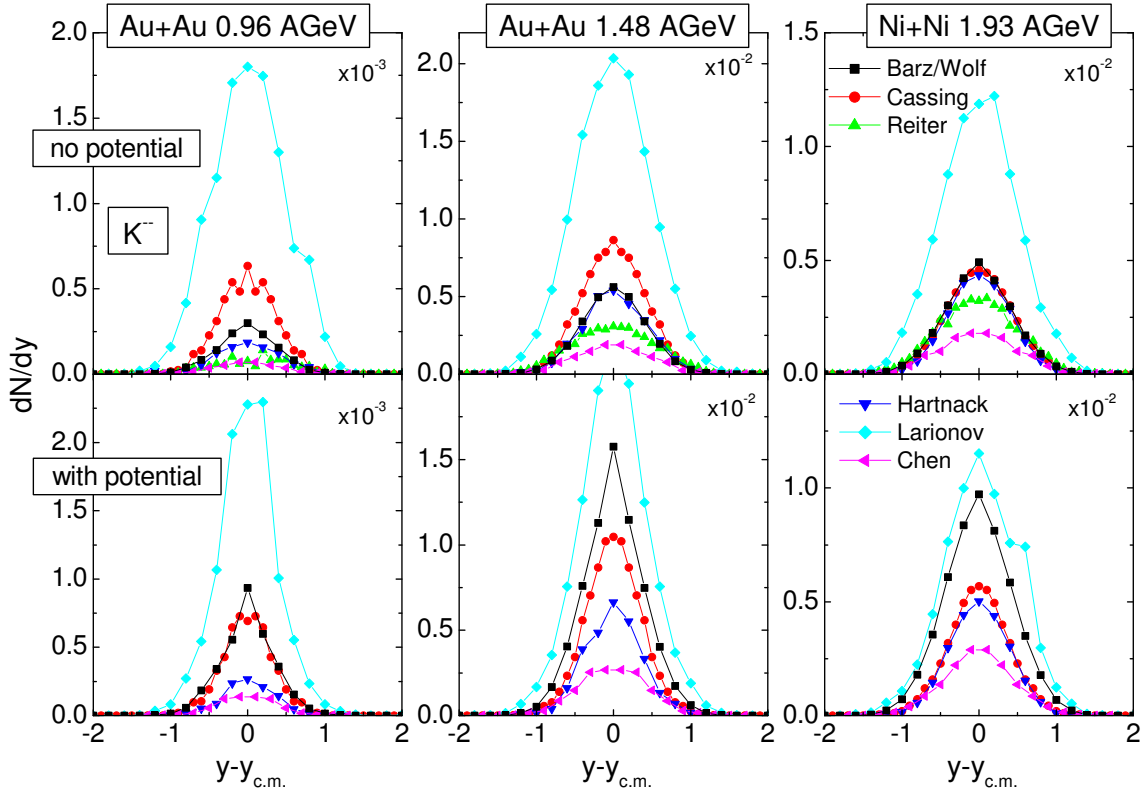


**Figure 11.** Final  $K^-$  rapidity distribution at  $b=1$  fm and with an enforced  $\Delta$  lifetime of  $1/120$  MeV (top row without, bottom row with  $KN$  potential) in the different approaches.

pointed in [40], due to the strange resonances this change is rather complex. In fact the detailed calculations [5], based on the well constrained  $KN$  interaction from [41], raise the question whether the  $K^-$  can still be treated as a quasi particle at high densities and temperatures. On the other hand, most of the observed  $K^-$  are produced not too far away from the surface and therefore the multiplicity should not be too much influenced by the kaon properties at high density. Currently, one has approached this problem by using the same form of the mean field potential as for the  $K^+$  with the parameters displayed in table 4. The energy  $\omega_{K^-}(k=0)$  decreases with increasing density and therefore one expects an increase of the  $K^-$  yield if the potential is switched on. This is indeed observed in the bottom figures of the figs.11 and 12. The enhancement seen when the  $K^-$  potential is switched on is different in the different approaches. An important part of this difference comes from different extrapolations of the known  $K^-N$  cross section, which diverges at small relative momenta to the  $\sqrt{s} < \sqrt{s_{\text{threshold}}}$  region. A solid theoretical basis for this extrapolation, which is necessary because the mass of the  $K^-$  decreases and hence the threshold is lowered, is not at hand presently.

## 8. Lasting results

One of the most challenging motivations for studying heavy ion collisions has been the search for the amount of energy which is needed to compress hadronic matter. This went under the slogan "Search of the nuclear equation of state". Earlier ideas to use pions or the in-plane flow of baryons as an experimental signal for the compressibility of matter, have not led to unambiguous results. The pions turned out to be not sensitive because most of them are produced when the system has already expanded to a low density. The in-plane flow is small at densities reachable in these reactions and it depends on the pressure which is proportional to the density gradient. Nuclear surface properties, like density gradients, are in general much more difficult to simulate than bulk properties.

It has been proposed to use  $K^+$  for this purpose because at these subthreshold energies they

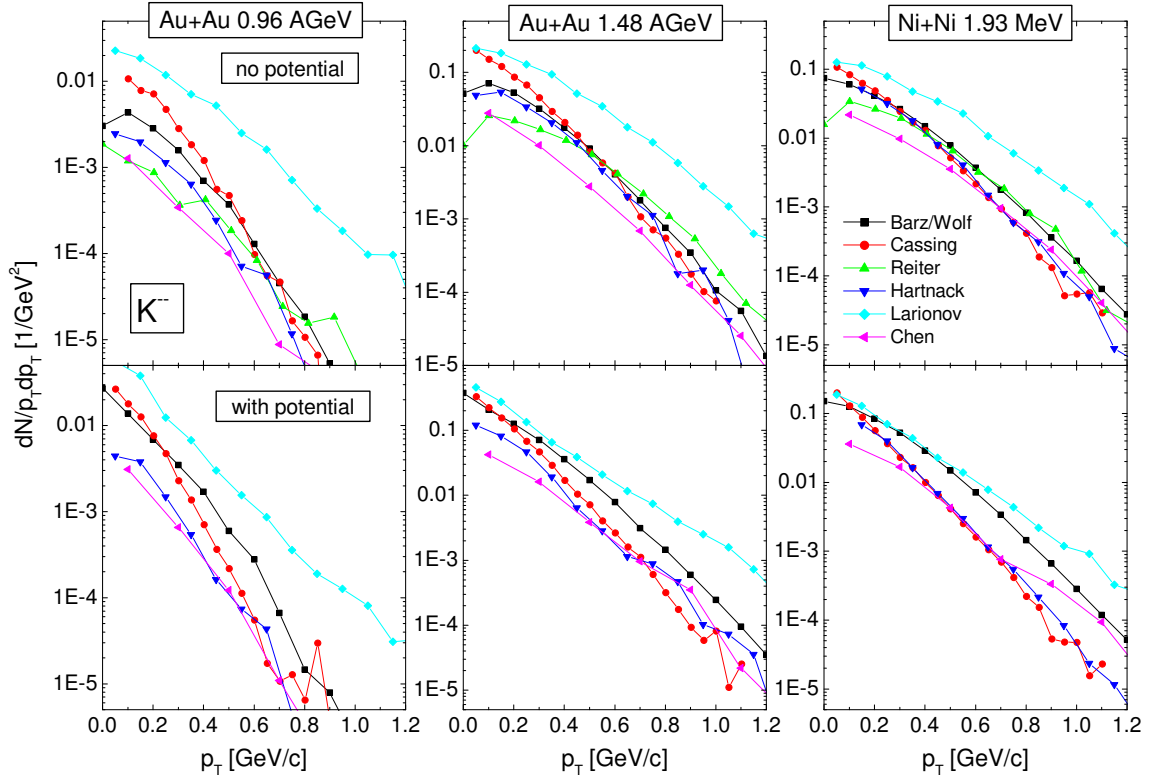


**Figure 12.** Final  $K^-$  transverse momentum distribution at  $b=1$  fm,  $|y_{cm}| < 0.5$  and with an enforced  $\Delta$  lifetime of  $1/120$  MeV (top row without, bottom row with KN potential) in the different approaches.

test the nuclear environment prior to production [42]. To get rid of many of the uncertainties it has been proposed by the KaoS collaboration [43] to use not the absolute yield but to compare a heavy with a light system where compression is virtually absent. Indeed, one has found that the excitation function of this ratio is rather sensitive to the compressibility of the nuclear potential and that the experimental results point strongly towards a nuclear potential with a compressibility  $\kappa \leq 280$  MeV. Such a potential has usually been dubbed as the "soft equation of state". In the meantime, one has tested whether this result is robust, i.e. whether it remains valid if one varies the unknown or little known input such as the  $\Delta$  lifetime or the  $\Delta N \rightarrow K^+$  cross section with the conclusion that only a strongly density dependent  $K^+$  production cross section may invalidate this result. Such a cross section, however, has never been proposed in elementary calculations. To which degree this result is stable against a change of the  $\Delta N \rightarrow K^+$  cross section is shown in the left panel of fig. 13 where the different cross sections vary by a factor of 2. The results appear fairly robust. One should stress, though, that we find here that nuclear matter is relatively easy to compress. The compressibility is compatible with the results obtained by analyzing giant resonances, i.e. the compression of nuclei at very low temperature and around the equilibrium density. However, the reactions discussed here yield high densities and temperatures and the system contains mesons and resonances. Thus we test here a completely different region in the  $T$ - $\rho$  plane.

## 9. Conclusion

Multiplicity, rapidity and transverse momentum distributions from different programs simulating heavy ion reactions at kinetic energies of around 1 AGeV have been compared. If the same inputs are used, the programs yield quite similar results but differ in details. Some of the differences are understood in terms of the implementation of different physical approaches in the programs, and others, less important, remain to be explained. Despite of these differences the programs agree on some important physical results: The pions are almost exclusively produced by resonance

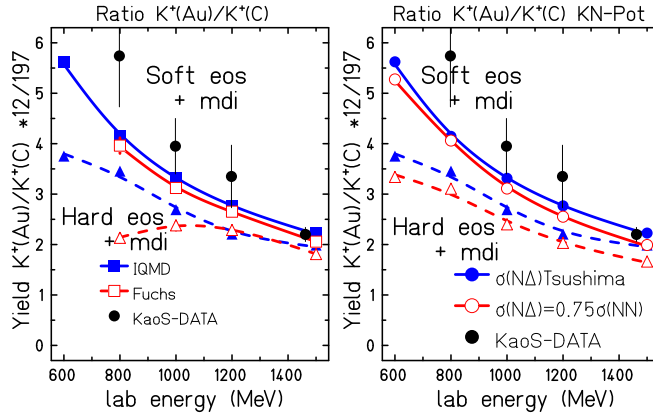


**Figure 13.** Normalized ratio of the  $K^+$  yield in Au+Au to C+C reactions as a function the beam energy for two different equations of states. Filled circles with errors represent the data of the KaoS collaboration [43]. Other symbols with lines represent calculations of ref. [21] on the left panel and of ref. [19] on the right panel for either the  $\Delta N \rightarrow K^+$  cross section of ref.[27] or for  $(\sigma(\Delta N \rightarrow K^+) = 3/4 \sigma(NN \rightarrow K^+))$  employed earlier.

decay. Subthreshold meson production is due to the same reaction as in free space and becomes possible because at least one of the collision partners has gained energy in collisions before. They programs furthermore agree on the stopping of matter, the dependence of the  $K^+$  squeeze out on its in-medium potential and on the softness of the density dependence of the effective nuclear potential.

*Acknowledgment* We would like to thank Dr. H. Oeschler for many valuable discussions and the *ECT\** in Trento, Italy, for hosting a workshop which was the starting point of this comparison.

## References

- [1] Y. Yariv and Z. Fränkel, Phys. Rev. **C20** (1979) 2227
- [2] J. Cugnon Phys. Rev. **C22** (1980) 1885
- [3] J. Aichelin and G. Bertsch Phys. Rev. **C31** (1985) 1730
- [4] H. Kruse, B.V. Jacak, J.J. Molitoris, G.D. Westfall, and H. Stöcker Phys. Rev. **C31**, (1985) 1770
- [5] M.F.M. Lutz and C.L. Korpa, Nucl. Phys. **A700** (2002) 309.
- [6] J. Lehr, H. Lenske, S. Leupold, U. Mosel, Nucl. Phys. **A703** (2002) 393  
M. Post, S. Leupold, U. Mosel, Nucl.Phys. **A741** (2004) 81
- [7] Yu. B. Ivanov, J. Knoll, D. N. Voskresensky, Nucl. Phys. **A672** (2000) 313
- [8] W. Cassing, S. Juchem, Nucl. Phys. **A665**, 377 (2000) and **A672**, 417 (2000)  
W. Cassing et al., Nucl. Phys. **A727** (2003) 59
- [9] Ch. Fuchs et al., Phys. Rev. **C67** (2003) 025202
- [10] L. Tolos et al., Phys. Rev. **C65** (2002) 054907
- [11] Gy. Wolf, W. Cassing, and U. Mosel, Nucl. Phys. **A552** (1993) 549  
Gy. Wolf, Heavy Ion Physics 5 (1997) 281  
H.W. Barz and L. Naumann, Phys. Rev. **C68** (2003) 041901(R)
- [12] W. Cassing and E. Bratkovskaya, U. Mosel, S. Teis and A. Sibirtsev, Nucl. Phys. **A614** (1997) 415
- [13] E. Bratkovskaya, W. Cassing, U. Mosel, Nucl.Phys **A622** (1997) 593  
W. Cassing and E. Bratkovskaya, Phys. Rep. **308** (1999) 65
- [14] M. Effenberger, E.L. Bratkovskaya, and U. Mosel, Phys. Rev. **C60**, (1999) 44614  
M. Effenberger, PhD thesis, Uni. Giessen, 1999,  
<http://theorie.physik.uni-giessen.de/html/dissertations.html>.

J. Schaffner-Bielich, V. Koch, M. Effenberger,,*Nucl. Phys.* **A669**, (2000) 153  
 A.B. Larionov and U. Mosel, in preparation.

[15] P. Danielewicz and G. Bertsch, *Nucl. Phys.* **A 533** (1991) 712

[16] C.M. Ko and G.Q. Li, *J. Phys. G* **22**, (1996) 1673  
 G.Q. Li, C.H. Lee, and G.E. Brown, *Nucl. Phys.* **A625**, (1997) 372  
 G.Q. Li, C.M. Ko, and W.S. Chung, *Phys. Rev.* **C57**, (1998) 434  
 C.M. Ko, Q. Li, and R. Wang, *Phys. Rev. Lett.* **59**, (1987) 1084  
 C.M. Ko and Q. Li, *Phys. Rev.* **C37**, (1988) 2270  
 Q. Li, J.Q. Wu, and C.M. Ko, *ibid.* **39**, 849 (1989); C.M. Ko, *Nucl. Phys.* **A495** (1989) 321c

[17] T. Gaitanos, C. Fuchs, H.H. Wolter, *Nucl. Phys.* **A650** (1999) 97  
 T. Gaitanos, C. Fuchs, H.H. Wolter, A. Fässler, *Eur. Phys. Journ.* **A12** (2001) 421

[18] J. Aichelin, *Phys. Rep.* **202** (1991) 233

[19] Ch. Hartnack et al., *Eur. J. of Nucl. Phys.* **A1** (1998) 151.  
 C. Hartnack, L. Zhuxia, L. Neise, G. Peilert, A. Rosenhauer, H. Sorge, J. Aichelin, H. Stöcker, and W. Greiner, *Nucl. Phys.* **A495** (1989) 303

[20] M. Bleicher *et al.*, *J. Phys. G* **25** (1999) 1859  
 S.A. Bass et al, *Prog. Part. Nucl. Phys.* **41** (1998) 225

[21] K. Shekhter, C. Fuchs, A. Fässler, M.I. Krivoruchenko, B.V. Martemyanov, *Phys. Rev.* **C68** (2003) 014904.  
 C. Fuchs et al., *Phys. Rev.* **C59** (1997) 12606  
 Y.-M. Zheng et al., *Phys. Rev.* **C69** (2004) 034907 C. Fuchs, A. Fässler, E. Zabrodin, Y.M. Zheng, *Phys. Rev. Lett.* **86** (2001) 1974  
 C. Fuchs, D. Kosov, A. Fässler, Z.S. Wang and T. Waindzoch, *Phys. Lett.* **B434** (1998) 254.

[22] FOPI Collaboration: W. Reisdorf, et al. *Phys. Rev. Lett.* **92** (2004) 232301

[23] T. Ericson and W. Weise, *Pions and Nuclei*, Oxford Science Publications, Clarendon Press, Oxford (1988)

[24] E. P. Wigner, *Phys. Rev.* **98** (1955) 145

[25] P. Danielewicz and S. Pratt, *Phys. Rev.* **C53** (1996) 249

[26] P. Senger, H. Ströbele, *J. Phys.* **G25** (1999) R59

[27] K. Tsushima *et al.*, *Phys. Rev.* **C59**, (1999) 369

[28] S. Sewerin et al., *Phys. Rev. Lett.* **83** (1999) 682

[29] M. Büscher, *Acta Phys. Polon.* **B35** (2004) 1055-1066, *nucl-ex/0311018*

[30] A. Sibirtsev, *Phys. Lett. B* **359**, (1995) 29

[31] T. Muto and T. Tatsumi, *Phys. Lett. B* **283** (1992) 165;  
 M. Lutz, A. Steiner, and W. Weise, *Nucl. Phys.* **A574** (1994) 755.

[32] Z. Rudy, W. Cassing, L. Jarczyk, B. Kamys, P. Kulessa, *Eur. Phys. J.* **A15** (2002) 303 and *nucl-th/0411009*

[33] M. Büscher et al., *nucl-ex/0401031*, accepted for publication in *EPJ A*

[34] G.Q. Li, C.M. Ko, and G.E. Brown, *Phys. Lett.* **B381** (1996) 17

[35] C. M. Ko , *Phys. Lett.* **B120** (1983) 294

[36] E.E. Kolomeitsev, D.N. Voskresensky, and B. Kämpfer, *Int. J. Mod. Phys. E* **5** (1996) 316.

[37] C. Hartnack, H. Oeschler and Jörg Aichelin, *Phys. Rev. Lett.* **90** (2003) 102302

[38] J. Cleymans et al, *Phys. Lett.* **B603** (2004) 146

[39] A. Förster, F. Uhlig et al. *Phys. Rev. Lett.* **91** (2003) 152301

[40] E.E. Kolomeitsev, D.N. Voskresensky, and B. Kämpfer, *Nucl. Phys.* **A588** (1995) 889.

[41] M.F.M. Lutz and E.E. Kolomeitsev, *Nucl. Phys.* **A700** (2002) 193.

[42] J. Aichelin and C.M. Ko, *Phys. Rev. Lett.* **55** (1985) 2661

[43] C. Sturm et al. (KaoS Collaboration), *Phys. Rev. Lett.* **86** (2001) 39